Shock structures and bunching fronts in excitable reaction-diffusion systems

Chad T. Hamik and Oliver Steinbock*
Department of Chemistry and Biochemistry, Florida State University, Tallahassee, Florida 32306-4390
(Received 16 November 2001; published 8 April 2002)

We report experimental results on the dynamics of excitation waves in a modified Belousov-Zhabotinsky reaction. The waves in this system obey nonmonotonic dispersion relations. This anomaly induces the stacking of excitation fronts into patterns with stable interpulse distances. The stacking process creates either a traveling shock structure or a cascade of bunching events in which metastable wave packets are formed. The direction and the speed of the shock are explained in terms of a simple geometrical analysis. We also present experimental evidence for the corresponding instabilities in two-dimensional systems. Here, wave stacking generates atypical structures in the collision of target patterns and wave bunching is accompanied by complex front deformations.

DOI: 10.1103/PhysRevE.65.046224 PACS number(s): 05.45.−a, 82.40.Ck

I. INTRODUCTION

Excitable systems reveal a wealth of spatiotemporal structures that have fascinated scientists for several decades [1,2]. Classic examples of these dissipative patterns include rotating spiral waves [3] and stationary Turing patterns [4]. The point dynamics of excitable systems is characterized by the existence of at least one steady state that is locally stable but susceptible to perturbations that exceed a particular threshold value [5]. In response to a sufficiently strong perturbation, the systems carry out a long excursion through phase space before they eventually return to the (newly excitable) rest state. This type of temporal behavior in conjunction with appropriate transport processes can give rise to constant-amplitude pulses, which have been observed in a variety of experimental systems, such as catalytic surfaces [6], homogeneously catalyzed reaction media [1], aggregating slime mold colonies [7], single cells [8], and yeast extracts [9]. Dynamically closely related are waves of excitation in neuronal and cardiac tissue where pulses of electric activity provide the means for the rapid and undamped relay of information and control signals [5].

The dynamics and stability of wave trains in excitable systems is dictated by the underlying dispersion relation that describes the speed of an excitation pulse, c, as a function of the distance to its predecessor, λ [10]. In many experimental systems, the dispersion relation is a monotonically increasing function that approaches a constant speed c_0 for increasing values of λ [11]. This behavior is known as normal dispersion and implies that the solitary pulse is the only stationary solution. Accordingly, all wave trains increase their interpulse distances continuously, although this effect becomes less and less pronounced in the course of the process [12].

In contrast to this normal behavior, anomalous dispersion relations involve a single overshoot or damped oscillations that converge to a constant speed c_0 for increasing wavelengths λ [13]. Normal as well as anomalous dispersion arise if the stable homogeneous solution can be represented as a node in a set of ordinary differential equations (ODEs) describing the dynamics near the stationary solution in comoving coordinates [13]. If this state is a focus in the corresponding ODE system, the dispersion relation will typically oscillate in the limit of large interpulse spacing. Notice that the value c_0 equals the speed of the solitary pulse. In the case of anomalous dispersion, stable finite wave trains can exist for a discrete set of interpulse distances λ_i. The stability criteria for these distances are $c(\lambda_i)=c_0$ and $dc/d\lambda>0$, which assures that all pulses travel with the velocity of the leading front and that small perturbations to the relative pulse positions vanish [14–16]. The impact of these simple stability criteria on the transport of information through excitable media is remarkable, because wave trains in which the the interpulse distances equal λ_i are error correcting.

Dispersion relations with damped oscillations are known to exist in neuronal systems for which the phenomenon is referred to as supernormal excitability [17]. In addition, some indications for anomalous dispersion have been obtained in experiments on chemical waves that organize the aggregation of the cellular slime mold *Dictyostelium discoideum* [18]. More concrete evidence, however, is provided by recent studies on the reduction of NO with CO on Pt(100) surfaces [19] and the Belousov-Zhabotinsky (BZ) reaction [20,21]. The latter system involves the oxidation of an organic compound by bromate in acidic solution. Recently, we have shown that this system obeys nonmonotonic, nonoscillatory dispersion relations for a broad range of initial conditions, if the reaction is carried out with 1,4-cyclohexanedione (CHD) as the organic reactant [21,22]. Our experiments revealed accelerating pulses that are the hallmark of anomalous dispersion. Moreover, we observed the stacking of waves at particular interpulse distances that we identified as the stable distances λ_0 mentioned above.

Here, we present results on the dynamics of excitation pulses derived from experiments with pseudo-one- and two-dimensional CHD-BZ media [23]. In particular, we analyze the shocklike ''absorption'' of fast pulses into slow moving, stacked wave packets, and a more complex wave train instability in which the pulses bunch into numerous, metastable wave packets. To our knowledge, the concept of shocklike structures in wave patterns of excitable systems was first introduced by Howard and Kopell [24]. These authors

*Author to whom correspondence should be addressed.

found that reaction-diffusion systems have solutions in which there are rapid transitions in local wave number and frequency over a localized transition region. In the simplest case, these shocks manifest themselves in a localized change in pulse density (i.e., the number of pulses per unit length). Later, Horikawa [25] studied shock dynamics in a FitzHugh-Nagumo model and revealed a close relation to the shock wave solution of Burgers equation. Notice that our use of the term shock does not necessarily imply a strictly discontinuous solution.

II. EXPERIMENT

Our experiments are carried out with the ferroin-catalyzed Belousov-Zhabotinsky reaction using 1,4-cyclohexanedione as the organic substrate. The reagents are of the highest grade commercially available and used without further purification. The stock solutions are prepared from high-purity water. Most of our measurements involve ferroin and sulfuric acid at initial concentrations of 0.5 mmol/l and 2.0 mol/l, respectively. To approximate the conditions of spatially one-and two-dimensional systems, the BZ solutions are filled into thin capillary tubes (inner diameter 1.1 mm) or the gap between glass plates spaced at 0.5 mm, respectively. In contrast to the classical BZ reaction that employs malonic acid, no gaseous products and hence no undesired gas bubbles are generated in the oxidation of CHD [26]. The reaction system is kept at a constant temperature of $25\pm1\,^{\circ}\mathrm{C}$ and is illuminated with white light. The detection of the evolving wave patterns is performed with a monochrome charge-coupled-device camera. The optical contrast in the reaction medium arises from the different absorption spectra of the redox couple ferroin/ferriin. For further analysis, the video signals are digitized at a sampling rate of 0.5 Hz during the experiment.

III. ONE-DIMENSIONAL WAVE PATTERNS

Figure 1 illustrates the typical stacking dynamics of excitation waves in pseudo-one-dimensional CHD-BZ systems. The individual frames are time-space plots generated by piling up spatial absorption profiles at a constant sampling rate. The vertical and horizontal axes represent time and space, respectively. In these plots each excitation pulse generates a bright band that slopes according to the inverse velocity of the given pulse. The examples show slow leading pulses that are followed by numerous fast fronts, all of which propagate from the left to the right. As the fast pulses encounter the refractory tail of a slow predecessor, they abruptly decelerate to form a closely stacked wave packet that moves with the speed of the leading front. In this process, the wave packet increases in size, but maintains a constant spacing between its individual members. More importantly, Fig. 1 illustrates that the point at which the incoming fronts decelerate itself moves at a characteristic velocity. Because the density of pulses within the stable wave packet is significantly higher than in the approaching wave train, this point can be considered a shock structure. It should be emphasized that the dynamics shown in Fig. 1 are characteristic for excitable media

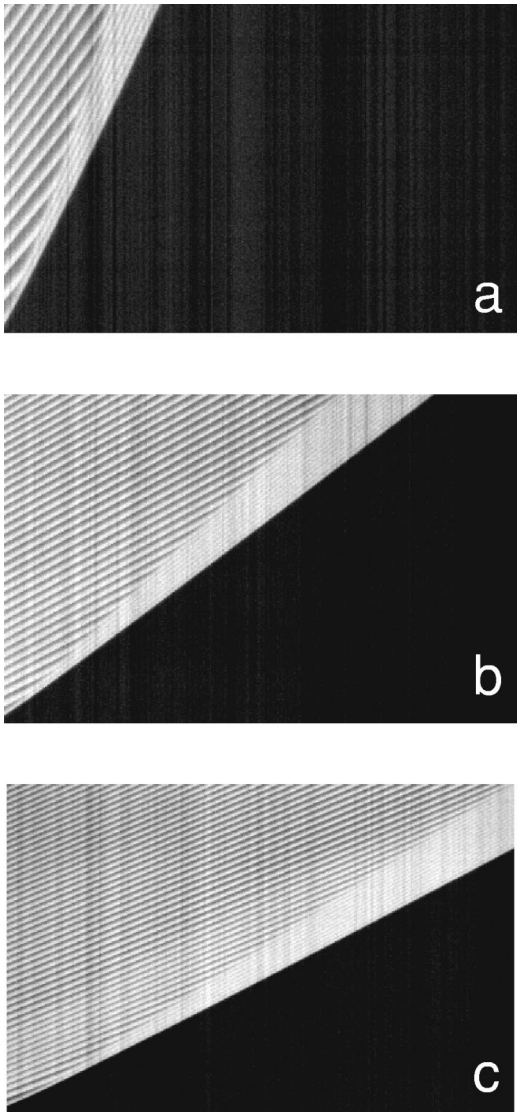

FIG. 1. Time-space plots of stacking excitation pulses. The dark background corresponds to the excitable, chemically reduced, state of the reaction medium, whereas the traveling pulses are represented by bright bands. The vertical and horizontal axes span 480 s and 40 mm, respectively, with time evolving in the upward direction. Initial concentrations: [ferroin] = 0.5 mmol/l, $[H_2SO_4]=2.0$ mol/l, $[CHD]=0.05$ mol/l (a), 0.13 mol/l (b), 0.19 mol/l (c), and $[NaBrO_3]=0.03$ mol/l (a), 0.09 mol/l (b), 0.14 mol/l (c).

with anomalous dispersion relations and do not occur in systems with normal dispersion.

The formation and propagation of the shock point are illustrated in the schematic drawing shown in Figure 2. Here, the motion of three excitation fronts and the resulting shock trajectory are depicted as solid and dashed lines, respectively. This simplified view of the real process assumes an instantaneous deceleration of the pulses as they are incorporated into the closely stacked wave packet. In the following, we denote the velocities of the leading pulse, the fast incoming wave train, and the shock point as c_0, c_1, and c_s, respectively. The interpulse spacings within the stacked wave packets and the fast wave train are referred to as λ_0 and λ_1,

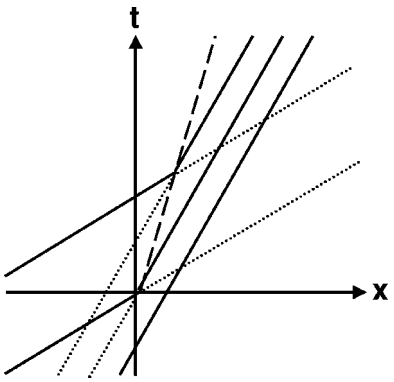

FIG. 2. Schematic drawing of the formation and propagation of a shock point during the abrupt deceleration of excitation pulses.

respectively. In the framework of the assumption above, straightforward calculus yields an expression for the velocity of the shock point:

$$c_s = \frac{c_0\lambda_1 - c_1\lambda_0}{\lambda_1 - \lambda_0}. \tag{1}$$

To evaluate the applicability of this equation to the pulse dynamics in the CHD-BZ system, we carried out numerous experiments for different sets of initial conditions. These experiments yielded a broad range of values for c_0, c_1, λ_0, and λ_1. The directly measured shock velocities span an interval between 1.0 and 5.6 mm/min. The resulting data are summarized in Fig. 3. The plot employs coordinates for which the experimental data are expected to show a proportional dependence (solid line). Despite the simplicity of our model, the data are in excellent agreement with Eq. (1), which indicates that the deceleration of the pulses is indeed very fast and not complicated by additional processes.

An interesting aspect of Eq. (1) is that it allows the formation of resting shock points and of shocks that move against the direction of the excitation pulses. The structure of

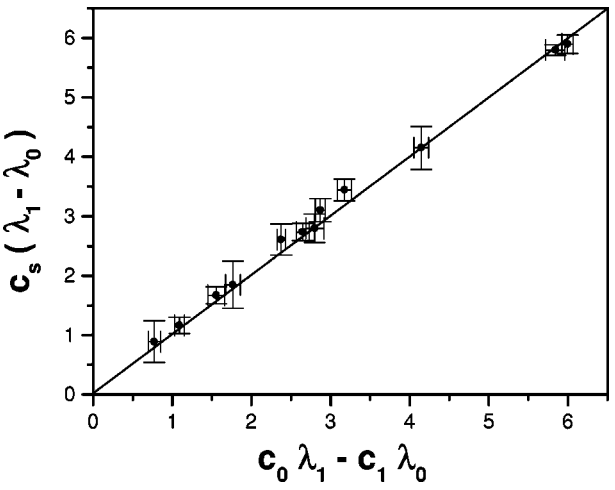

FIG. 3. Comparison of experimental data (solid circles) to the linear dependence (solid line) predicted by Eq. (1). Experiments are carried out for various initial concentrations of CHD (0.05 to 0.21 mol/l) and $NaBrO_3$ (0.03 to 0.14 mol/l).

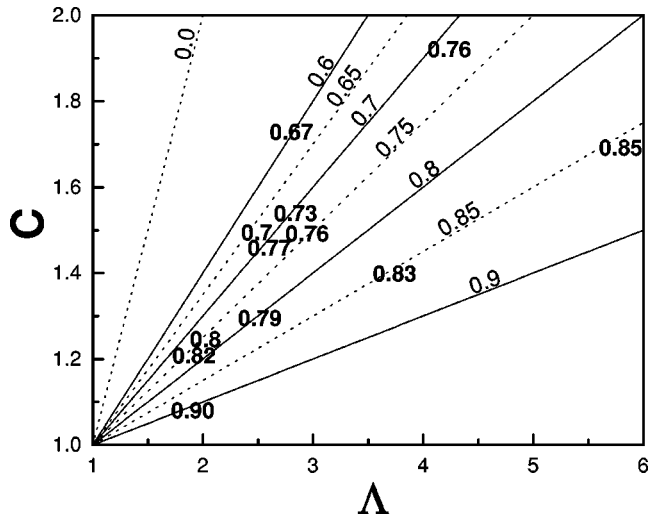

FIG. 4. Shock velocities (C_s) plotted in the plane of dimensionless pulse velocities and interpulse distances. Bold numbers indicate experimental results. Dotted and solid lines are obtained from Eq. (2).

the underlying dependence can be seen more easily by rewriting Eq. (1) in the dimensionless form

$$C_s = \frac{\Lambda - C}{\Lambda - 1}, \tag{2}$$

where $C_s = c_s/c_0$, $C = c_1/c_0$, and $\Lambda = \lambda_1/\lambda_0$. For $\Lambda > 1$, this expression indicates the existence of three main cases that can be summarized as follows: (a) the excitation pulses and the accompanying shock point propagate in the same direction ($\Lambda > C$); (b) the shock point rests, although the pulses are moving ($\Lambda = C$); (c) the excitation pulses and the shock point propagate in opposite directions ($\Lambda < C$). The examples shown in Fig. 1 belong to the case (a) and up to now we could not obtain any convincing evidence for resting or backward traveling shocks in the CHD-BZ system. Nevertheless, one must consider that the cases (b) and (c) are difficult to observe in our experiments, because the excitation pulses nucleate from a small, resting pacemaker. In the framework of instantaneously decelerating pulses (Fig. 1), the shock point would therefore be identical to the location of the pacemaker, if $\Lambda \leqslant C$. Hence, the experimental analysis of resting and/or backward propagating shocks would require the design of an experiment in which the velocities of the excitation pulses are externally perturbed in the course of the reaction. In the simplest case, this could be achieved by a sudden change in the system's overall temperature or by the utilization of the reaction's photosensitivity [26]. In this study, we have not attempted to realize this particular type of experiment. However, some conclusions regarding the presence or absence of the $\Lambda \leqslant C$ scenario can be drawn from the data discussed below.

The plot in Fig. 4 shows 12 dimensionless shock velocities (bold numbers) according to their location in the (Λ, C) plane. The experimental data are complemented by several lines that correspond to the function $C = \Lambda - C_s(\Lambda - 1)$ [see Eq. (2)] at different values of C_s. These values range be-

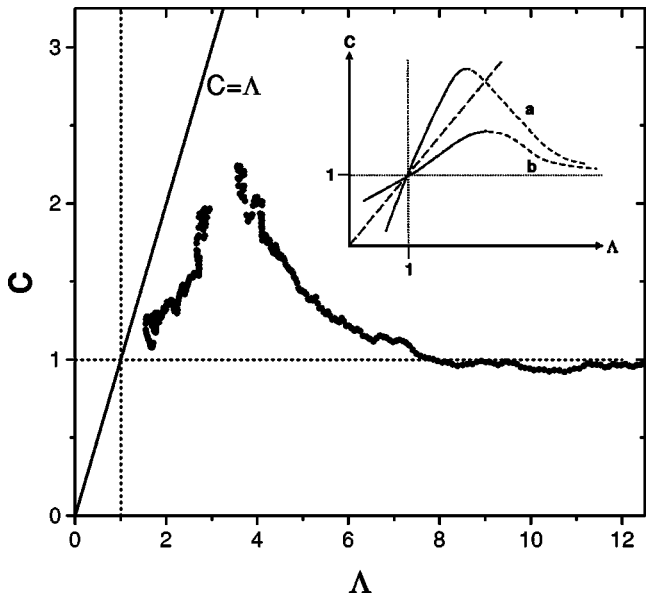

FIG. 5. Dispersion relation of stacking pulses in the CHD-BZ reaction in terms of the dimensionless pulse speed C and interpulse distance Λ. The initial concentrations of CHD, $NaBrO_3$, H_2SO_4, and ferroin are 0.15 mol/l, 0.1 mol/l, 2.0 mol/l, and 0.5 mmol/l, respectively. The inset shows a schematic drawing of two anomalous dispersion relations. Only curve *a* will allow the formation of backward propagating shocks.

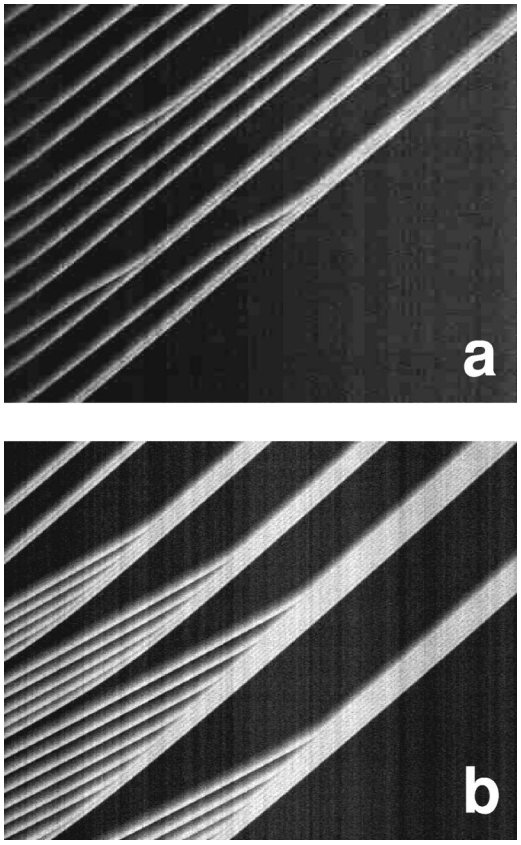

FIG. 6. Time-space plots of wave trains that bunch into clusters of stable wave packets. The vertical and horizontal axes span 480 s and 40 mm, respectively, with time evolving in the upward direction. The initial concentrations of CHD, $NaBrO_3$, H_2SO_4, and ferroin are 0.15 mol/l, 0.1 mol/l, 2.0 mol/l, and 0.5 mmol/l, respectively.

tween 0.0 and 0.9 and are denoted as tilted numbers. The experimental results are in good agreement with Eq. (2), although some of the lower values seem to be underestimated by the theoretical expression. Notice that resting and backward propagating shock points are characterized by $C_s=0$ and $C_s<0$, respectively. However, the lowest shock velocity C_s that we could measure reliably in our experiments is approximately 0.6 and no evidence for velocities below 0.3 was found.

The results above reveal an important connection between the shocklike structures and the underlying anomalous dispersion relation of the excitable medium. Figure 5 shows a dispersion curve obtained from the transient interaction of stacking excitation pulses in the CHD-BZ system [21]. The experimental data are rescaled to the dimensionless variables C and Λ and complemented by a schematic drawing of two nonmonotonic, nonoscillatory dispersion curves. A necessary criterion for the existence of non-forward-moving shocks is that the dispersion curve intersects the $C=\Lambda$ line for $\Lambda>1$. This scenario is exemplified by the curve *a* in the inset of Fig. 5, whereas curve *b* describes a system in which shocks and pulses always propagate in the same direction. The measured dispersion relation is found to stay below the critical $C=\Lambda$ boundary. All of these findings indicate that the experimental conditions for non-forward-moving shocks are either hard to find or nonexisting in the CHD-BZ reaction. Moreover, we should mention that the analogous cases for $\Lambda<1$ might imply the destacking of wave trains in shocklike processes.

The existence of sustained shock structures is subject to an additional limitation that arises from a wave train instability known as pulse bunching. This instability affects only wave trains in which the interpulse distance is on the downsloping branch of the dispersion curve (dashed curve segments in the inset of Fig. 5). Two typical examples of this bunching instability in pseudo-one-dimensional CHD-BZ systems are shown in Fig. 6.

The bunching instability was first described in theoretical studies by Rinzel and co-workers [12,13]. It involves the decay of a wave train into various wave packets that consist of individual pulses spaced at a stable distance (λ_0). This process occurs as a cascade of bunching events in which the spatial separation between neighboring clusters increases to less unstable distances. In the CHD-BZ system, the resulting metastable patterns can have remarkably long lifetimes, but it is expected that they will eventually generate a single wave packet in which all pulses are stacked in a stable fashion. The bunching instability applies an additional constraint on the existence of persistent shock structures. Nonetheless, smaller segments of a bunching wave train can show intermittent sequences of shock propagation as exemplified by the cluster formation in Fig. 6(b).

IV. TWO-DIMENSIONAL WAVE PATTERNS

The stacking of excitation pulses as well as the formation of the accompanying shock structures is not limited to one-

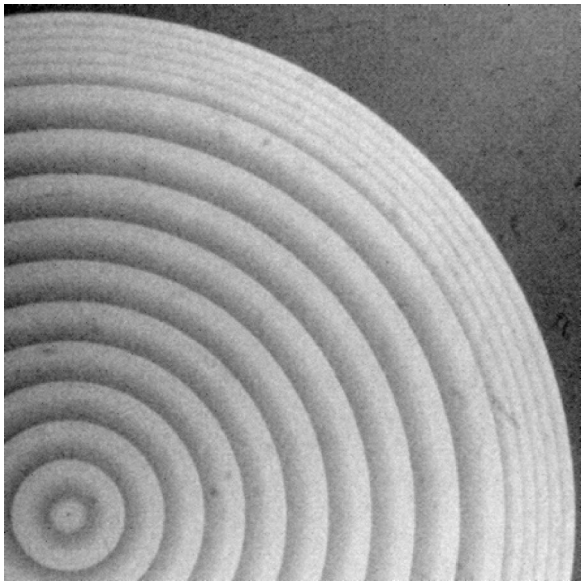

FIG. 7. Stacking of circular pulses within a target pattern. The initial concentrations of $NaBrO_3$, CHD, H_2SO_4, and ferroin are 0.07 mol/l, 0.11 mol/l, 2.0 mol/l, and 0.5 mmol/l, respectively. Field of view: 20×20 mm^2.

dimensional systems. Figure 7 shows a snapshot of a typical target pattern in the CHD-BZ reaction. The leading front of this expanding, two-dimensional wave pattern propagates at a slow speed of 3.6 mm/min, whereas faster pulses (5.8 mm/min) are found around the pacemaker at the lower left corner of the figure. At the time of data acquisition, the five outermost excitation pulses had already stacked at an interpulse distance of 0.44 mm. In the course of the reaction, additional pulses were incorporated into the expanding annulus of closely stacked fronts. The resulting shock line is a circle centered around the pacemaker of the target pattern. Its radial velocity (2.8 mm/min) equals the shock speed expected for the analogous pseudo-one-dimensional system. Consequently, Eqs. (1) and (2) can be applied for the description of this highly symmetric wave pattern.

Figure 8 presents an example of the effect of anomalous dispersion on the interaction between two-dimensional wave patterns. In this image sequence, two target patterns undergo successive wave collisions. As expected, the collisions occur on the line connecting the pacemakers [24]. The collision point shifts into the region of lower frequency and eventually wipes out the slow pacemaker [see Fig. 8(f)]. These dynamics are accompanied by the stacking of wave pulses at the leading front of the combined pattern. Each collision event creates a pair of cusp-shaped front segments that depart from the collision point in opposite directions. The cusps fall on a curve that bends into the high-frequency region. In contrast to systems with normal dispersion, these cusps disappear as they become part of the stacked wave packet [see white arrow in Fig. 8(e)]. In addition, a new cusp forms along the front which in turns acquires the geometry of the leading wave pulse. Consequently, the rim of stacked pulses has a consistent shape that is determined solely by the front geometry created in the very first collision. Notice that this master front also affects the shape of waves generated after the annihilation of the low-frequency pacemaker.

As described above, one-dimensional wave trains can undergo complex cascades of bunching events, if their interpulse distance is on the unstable branch of the dispersion curve (i.e., $dc/d\lambda<0$). In the following, we present evidence for this bunching instability in systems with two spatial dimensions. The image sequence in Fig. 9 shows the upper right quadrant of a target pattern and its cascading decay into complex pulse clusters. Additional, high-frequency wave trains enter the field of view from three directions. In Fig. 9(a), the target pattern consists of nearly circular wave fronts and the radial symmetry is not yet affected. However, this early snapshot already shows the first signs of pulse bunching, as exemplified by the relatively large distances between some of the wave fronts. Approximately 30 s later [Fig. 9(b)], two fronts have formed a smooth wave packet, but the subsequent pulses experience deformations of their initially circular shape. In the course of time, the deformations grow in amplitude and give rise to the wiggled fronts shown in Fig. 9(c).

The last results provide insights into the dynamics of bunching waves in two-dimensional CHD-BZ systems. They reveal that the bunching instability affects not only the radial interpulse spacing, but also the lateral degrees of freedom.

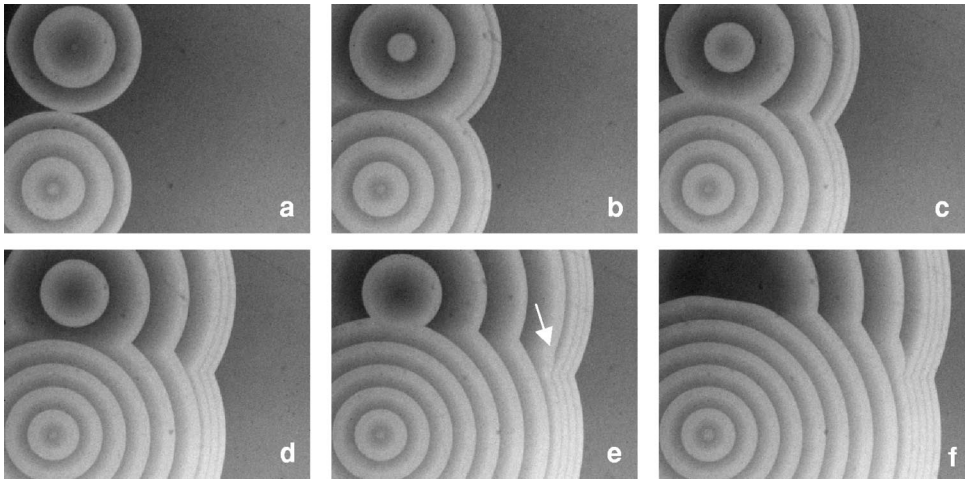

FIG. 8. Colliding waves of target patterns in the CHD-BZ reaction. Time between snapshots: 120 s. The initial concentrations of $NaBrO_3$, CHD, H_2SO_4, and ferroin are 0.07 mol/l, 0.11 mol/l, 2.0 mol/l, and 0.5 mmol/l, respectively. Field of view: 20×15 mm^2.

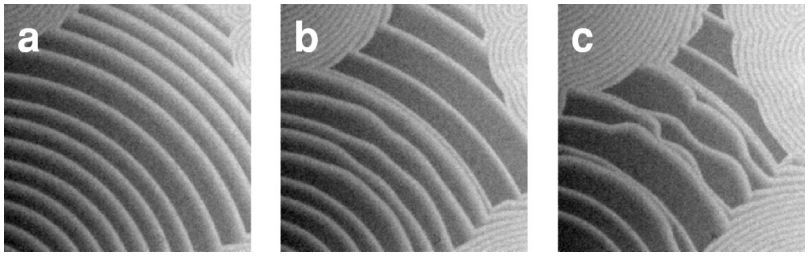

FIG. 9. Typical example for wave bunching in two-dimensional CHD-BZ systems. Time between snapshots: 30 s. The initial concentrations of $NaBrO_3$, CHD, H_2SO_4, and ferroin are 0.14 mol/l, 0.25 mol/l, 2.0 mol/l, and 0.5 mmol/l, respectively. Field of view: 20×20 mm^2.

Our observations suggest that different angular segments of the unstable wave train begin to undergo different sequences of bunching events. This inhomogeneity reflects the sensitivity of the unstable wave pattern to minute perturbations such as might arise from intrinsic fluctuations and/or the high-frequency waves at the edges of Fig. 9. However, along a given front the bunching sequences cannot develop independently, because the resulting front deformations alter the local velocities according to the well-known eikonal equation [27] and cause changes in the normal directions of the fronts. This coupling induces bumpy wave fronts along which the deformations can propagate in lateral direction. Recently, Steinbock reported a related phenomenon for the front dynamics in the wake of planar wave pulses [28]. In numerical simulations, it was shown that oscillatory dispersion can give rise to stationary solutions that embrace various sigmoidal front geometries. Their inflection point travels in the lateral direction and mediates transitions between different, stable interpulse distances. In our experiments, however, only one stable distance exists and long wavelengths are metastable. This difference might contribute to the complexity of the front geometries shown in Fig. 9(c).

V. CONCLUSIONS

Our experiments demonstrate the existence of constant-speed shock structures in one- and two-dimensional CHD-BZ media. The shock propagates in the forward direction and its velocity can be predicted from a simple geometrical analysis. Nonetheless, this analysis allows for backward traveling shocks, if the overshoot of the dispersion curve is sufficiently large. An experimental demonstration of reverse shock propagation would be interesting because the phenomenon implies the transport of information against the direction of wave propagation. More complex dynamics are observed for wave trains with long interpulse distances. These undergo an instability that generates metastable wave packets in a cascade of bunching events. In two-dimensional media, the bunching instability also affects the shape of the front curves and generates laterally moving deformations. Although our experimental results are obtained exclusively from the excitable CHD-BZ reaction, they are most likely characteristic for many excitable systems with anomalous dispersion, such as certain surface reactions and various biological media [18,19]. The comprehensive analysis of this class of reaction-diffusion systems is therefore an important challenge for future investigations. In particular, it will be interesting to study the impact of anomalous dispersion on the encoding and transport of information. Recent neurophysiological studies provide growing evidence for neuronal codes that go beyond the classic integrate-and-fire scheme by directly utilizing the interpulse distances of action potentials [29]. For example, it was shown that neurons in the peripheral auditory system can encode information on the basis of individual pulse intervals [30]. From a more general point of view, these nontraditional codes raise fundamental questions regarding the stability and dynamics of patterned wave trains. We believe that the investigation of the CHD-BZ system will provide useful insights into these intriguing aspects of excitable systems.

ACKNOWLEDGMENTS

This work was supported by the Florida State University.

[1] *Chemical Waves and Patterns*, edited by R. Kapral and K. Showalter (Kluwer, Dordrecht, Netherlands, 1995).
[2] V.K. Vanag and I.R. Epstein, Science **294**, 835 (2001).
[3] A.T. Winfree, Science **175**, 634 (1972); O. Steinbock, V. Zykov, and S.C. Müller, Nature (London) **366**, 322 (1993).
[4] V. Castets, E. Dulos, J. Boissonade, and P. De Kepper, Phys. Rev. Lett. **64**, 2953 (1990); Y.J. Li, J. Oslonovitch, N. Mazouz, F. Plenge, K. Krischer, and G. Ertl, Science **291**, 2395 (2001).
[5] J.D. Murray, *Mathematical Biology* (Springer, New York, 1989).
[6] J. Wolff, A.G. Papathanasiou, I.G. Kevrekidis, H.H. Rotermund, and G. Ertl, Science **294**, 134 (2001).
[7] K.J. Lee, R.E. Goldstein, and E.C. Cox, Phys. Rev. Lett. **87**, 068101 (2001).
[8] L.F. Jaffe and R. Creton, Cell Calcium **24**, 1 (1998).
[9] S.C. Müller, T. Mair, and O. Steinbock, Biophys. Chem. **72**, 37 (1998).
[10] J.D. Dockery, J.P. Keener, and J.J. Tyson, Physica D **30**, 177 (1988).
[11] A. Pagola, J. Ross, and C. Vidal, J. Phys. Chem. **92**, 163 (1988); O. Steinbock and S.C. Müller, Physica A **188**, 61 (1992); J.M. Flesselles, A. Belmonte, and V. Gaspar, J. Chem. Soc., Faraday Trans. **94**, 851 (1998).
[12] J. Rinzel and K. Maginu, in *Nonequilibrium Dynamics in Chemical Systems*, edited by C. Vidal and A. Pacault (Springer, Berlin, 1984), pp. 107–113.
[13] C. Elphick, E. Meron, and E.A. Spiegel, Phys. Rev. Lett. **61**, 496 (1988); SIAM (Soc. Ind. Appl. Math.) J. Appl. Math. **50**,

490 (1990); C. Elphick, E. Meron, J. Rinzel, and E.A. Spiegel, J. Theor. Biol. **146**, 249 (1990).
[14] A.T. Winfree, Phys. Lett. A **149**, 203 (1990); Physica D **49**, 125 (1991).
[15] M.G. Zimmermann *et al.*, Physica D **110**, 92 (1997).
[16] M. Or-Guil, I.G. Kevrekidis, and M. Bär, Physica D **135**, 154 (2000).
[17] J.D. Kocsis, H.A. Swadlow, S.G. Waxman, and M.H. Brill, Exp. Neurol. **65**, 230 (1979).
[18] F. Siegert and C.J. Weijer, J. Cell. Sci. **93**, 325 (1989).
[19] J. Christoph, M. Eiswirth, N. Hartmann, R. Imbihl, I. Kevrekidis, and M. Bär, Phys. Rev. Lett. **82**, 1586 (1999).
[20] N. Manz, S.C. Müller, and O. Steinbock, J. Phys. Chem. A **104**, 5895 (2000).
[21] C.T. Hamik, N. Manz, and O. Steinbock, J. Phys. Chem. A **105**, 6144 (2001).
[22] An earlier study reported a supposedly ''inverse'' dispersion relation for the malonic acid–BZ reaction. These results, however, are questionable because they were derived from closed systems 1 h after the onset of the reaction without accounting for the total number of oxidation pulses that had passed through the medium. Hence, high- and low-frequency data were measured under significantly different conditions [W. Hanke, Int. J. Bifurcation Chaos Appl. Sci. Eng. **9**, 2099 (1999)].
[23] I. Szalai, E. Körös, and L. Györgyi, J. Phys. Chem. A **103**, 243 (1999); M. Orbán, K. Kurin-Csörgei; A.M. Zhabotinsky, and I.R. Epstein, J. Am. Chem. Soc. **120**, 1146 (1998).
[24] L.N. Howard and N. Kopell, Stud. Appl. Math. **56**, 95 (1977).
[25] Y. Horikawa, Physica D **82**, 365 (1995).
[26] K. Kurin-Csörgei, A.M. Zhabotinsky, M. Orbán, and I.R. Epstein, J. Phys. Chem. A **101**, 6827 (1997).
[27] A.S. Mikhailov, *Foundations of Synergetics I* (Springer-Verlag, Berlin, 1990); J.J. Tyson and J.P. Keener, Physica D **32**, 327 (1988).
[28] O. Steinbock (unpublished).
[29] Z.F. Mainen and T.J. Sejnowski, Science **268**, 1503 (1995); D. Ferster and N. Spruston, *ibid.* **270**, 756 (1995); M. Diesmann, M.-O. Gewaltig, and A. Aertsen, Nature (London) **402**, 529 (1999).
[30] C.E. Carr and M. Konishi, J. Neurosci. **10**, 3227 (1990).